Mem. S.A.It. Vol. 85, 570

Memorie della

Unravelling a complex system: the Fornax dwarf spheroidal galaxy

Andrés del Pino Molina, Sebastian L. Hidalgo, and Antonio Aparicio

[1] Universidad de La Laguna
[2] Instituto de Astrofísica de Canarias e-mail: adpm@iac.es

Abstract. We present the results of an extended photometrical study of the Fornax dwarf spheroidal (dSph) galaxy. Using wide field, deep photometry ($\sim 0.86(^\circ)^2$, V $\sim$ 24), we have studied the spatial distribution of the stellar content in Fornax. We found strong asymmetries and conspicuous features in younger populations ($t < 4$ Gyr). We also derived the full star formation history (SFH) and the age-metallicity relation (AMR) as a function of radius in three very deep FORS1@VLT fields. We found that the star formation (SF) began $\sim$ 10 Gyr ago, and finished very recently (<1 Gyr), showing significant differences as a function of radius. These results are consistent with spectroscopic data from CaT.

Key words. galaxies: evolution – Local Group – galaxies: dwarf – early Universe

1. Introduction

In the Λ-CDM scenario, dwarf galaxies are the building blocks from which larger galaxies are formed (e.g. Blumenthal et al. 1985). The dwarf galaxies we observe today may be surviving systems that have not yet merged with larger galaxies. Hence, their underlying structure may provide important clues about the process of dwarf galaxy formation at high redshifts.

The evolution and SFH of dwarf galaxies are determined by local processes such as supernovae feedback and tidal interactions with nearby systems, as well as by global "*cosmic environmental factors*" like the reionization of the Universe by UV-background (e.g. Kravtsov et al. 2004). From one side, these global and local mechanisms could be responsible for suppressing galaxy formation in dwarf halos, and may explain the so called "*missing satellites problem*" (e.g. Moore et al. 1999). On the other hand, these effects could be involved in the large variety of properties in terms of mass, gas content, SFH, and chemical evolution that we observe today in dwarf galaxies.

In the present work we present the full SFH, and the spatial distribution of the stellar populations of the Fornax dSph, one of the nine classic known dSph satellites of the Milky Way (MW). Fornax is a remarkable object of study. After the Sagittarius dSph, is the largest and most luminous of the spheroidal MW companions. These two galaxies are the only dSph satellites of the MW hosting globular clusters. Moreover, Fornax shows two conspicuous star clumps located at 17′ and at 1.3° from its centre. The origin of these structures still being subject of an ongoing debate.

2. Photometry and spectroscopy

Two different photometry sets were used (See Fig1). The first one consist on wide field pho-

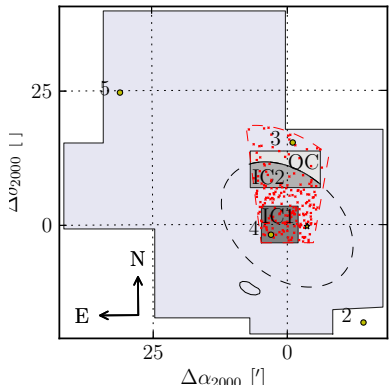

Fig. 1. Observed fields and the distribution of the CaT stars used for the spectroscopic AMR. Wide field photometry is marked in light blue. Regions used for the study of SFH gradients are shown in different gray shades and labeled accordingly. The dashed ellipse correspond to the core radius. Globular clusters are represented with yellow filled circles. The stellar clump found by Coleman et al. (2004) is also represented (17' southeast from the galaxy centre).

tometry ($\sim 0.9(^\circ)^2$) reaching V $\sim$ 23 (Stetson 2000, 2005). The large spatial coverage makes this photometry perfect for study spatial distribution of the stellar populations. The second data set is deep FORS1@VLT photometry covering three fields located one at the centre, and the other two $\sim 10'$ to the north. Reaching I $\sim$ 25, this photometry allow us to obtain its detailed SFH. Lastly, we count on a complete set of metallicities derived from low and medium resolution spectroscopy for red giant stars (for further information see del Pino et al. 2013). These stars allow us to obtain a independent AMR.

3. Methodology

3.1. Wide field photometry

The color magnitude diagram (CMD) of Fornax provides substantial information about its stellar populations. We computed a synthetic CMD (sCMD) corresponding to a stellar population created with constant star formation rate, and an uniform metallicity distribution within $Z = 0.001$ and $Z = 0.08$ over the full history of the galaxy (time from 0 to 13.5 Gyr). This sCMD was used as a model to define five macro-regions in the observed CMD, delimiting the evolutionary phases used in our analysis. The regions were created as shown in Figure 2: (1) the horizontal branch; (2) the red giant stars; (3) the sub-giants stars; (4) the young MS stars, and (5) the bluest and brightest stars of the main sequence.

Spatial distribution maps, were obtained by computing 2 dimensional histograms of the coordinates for stars within each defined CMD region. The density maps were convolved with a gaussian filter to reduce statistical noise.

3.2. Deep photometry and CaT stars

Deriving the SFH require of deep and precise photometry reaching at least 1 magnitude below the oldest main sequence turn off. We selected the stars of the deep photometry list attending to the galactocentric distance, defining three regions: IC1, IC2, OC (See Fig1). Using CMD-fitting techniques (Aparicio & Hidalgo 2009) we obtained the SFHs in the three regions. Futher details about the followed procedure can be found in del Pino et al. (2013).

In order to obtain the spectroscopic AMR, we selected the CaT stars within the elliptical section shown in Fig1, keeping a good statistical significance and avoiding spatial biases. We break the age-metallicity degeneracy by using polynomial relationships by Carrera et al. (2008).

4. Results

4.1. Spatial distribution

In Fig 3 we show the results of the spatial distribution of the stellar populations. Differences between populations are evident. We have found strong asymmetries in the young populations, with distributions which appear not to follow the orientation of the galactic axis, or even a spheroidal shape. Also noticeable is the shell previously detected by Coleman et al. (2004), which appear to be formed by young stars, i.e. stars aged between 0.5 and 4 Gyrs.

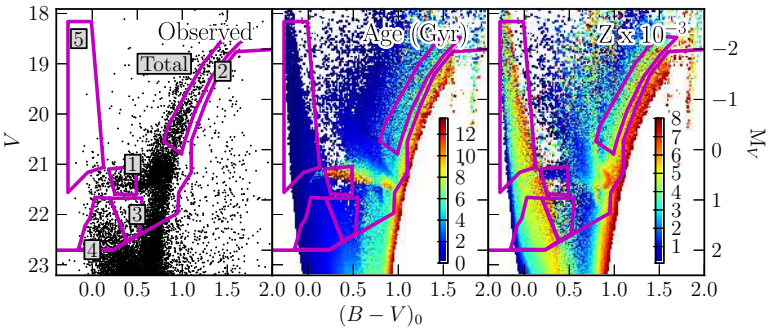

Fig. 2. Left: Sampled regions of the observed CMD (Only $\sim 1.5 \times 10^3$ stars showed). Middle: Expected mean age in the sCMD. Right: Expected mean metallicity in the sCMD.

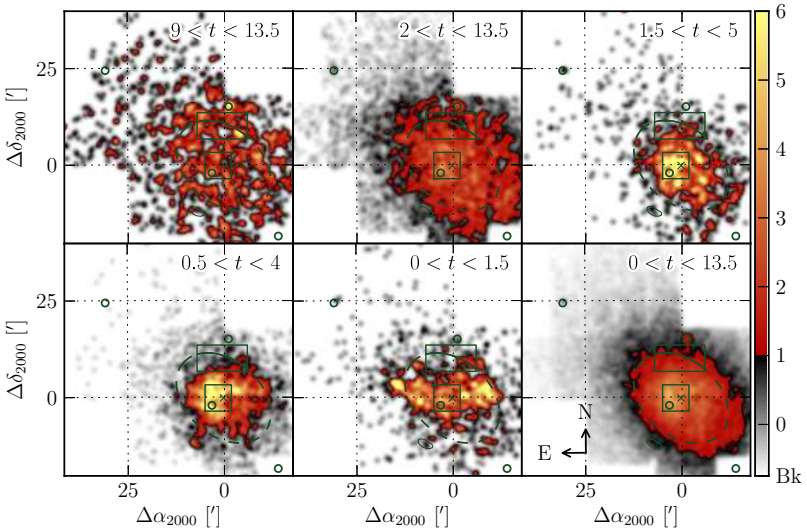

Fig. 3. Spatial distribution maps for the five defined populations in the CMD. Panels are ordered from old to young populations. Color scale is common for all panels, and indicates the concentration of stars normalized to the number of stars of each population. Levels are in units of standart deviation for each population.

The oldest stars are uniformly spreaded well beyond the core radius, while mid-aged stars follow the spheroidal shape defined by the core radius.

4.2. The star formation history

Figure 4 summarizes the main results of ths SFH of the Fornax dSph. The innermost region (IC1) has the youngest stellar population of three regions, formed mainly by intermediate age stars. In the outer regions (IC2, OC) the importance of recent SF episodes decrease gathering the bulk of their stars at old-intermediate ages. While outer regions shows a main burst occurred 10 Gyrs ago, the SF in IC1 peaks ∼2 Gyrs latter. The agreement between the spectroscopy based AMR and the one obtained us-

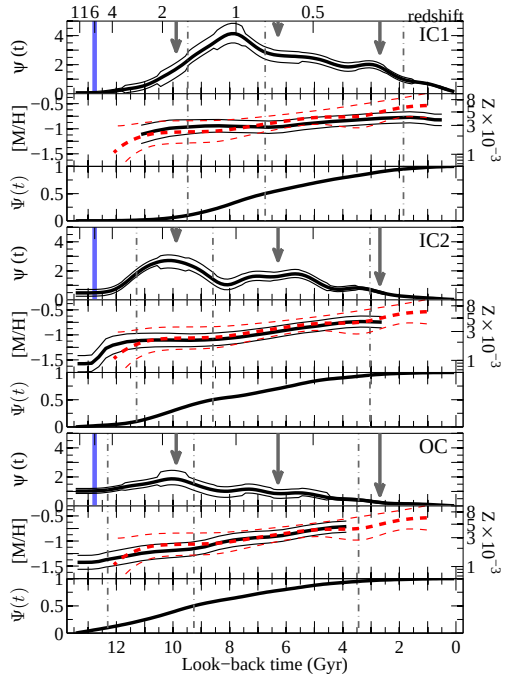

Fig. 4. Star formation rate as a function of time, $\psi(t)$, in units of $10^{-9}M_{\odot}yr^{-1}pc^{-2}$ (upper panel), age-metallicity relation (middle panel), and the cumulative mass fraction, $\Psi(t)$, (bottom panel) of each region. Errors are drawn by thin lines. Plots are ordered from top to bottom: IC1, IC2, and OC respectively. Units of $\psi(t)$ are normalized to the corresponding region area. 10th,50th, and 95th-percentile of $\Psi(t)$ are drawn with dash-dotted vertical lines. Reionization era is marked at $z \sim 6$ in blue. The AMR obtained from CaT spectroscopy is represented by a red-dashed line. Possible passes of Fornax through it perigalacticon, derived from the orbital parameters by Piatek et al. (2007), are represented by vertical arrows.

ing photometry is very good in general, in all the cases.

5. Conclusions

Fornax is a very complex system. It started its SFH approximately 10-11 Gyrs ago. This first stellar population, appears to follow a a spheroidal distribution, extending far beyond the core of the galaxy. Young stars are concentrated within the core, showing important asymmetries in its distribution.

This can be also observed in the SFH of Fornax. The centermost region (IC1) has kept an efficient star formation (SF) until recently, showing a widely spread metallicity range on their stars, as an important young population. In the outer regions, these last SF episodes were of little significance, leaving old metal-poor stars as the dominant population in the outskirt of the galaxy.

Neither Universe reionization, nor supernovae feedback appear to have a determining effect on Fornax. Interactions with other systems have been also taken into account. Using the orbital parameters from Piatek et al. (2007), we have estimated the passages of Fornax through its perigalacticon. A relation between SF enhancements and perigalacticon passages is not clear, although can not be ruled out. On another hand, the strong asymmetries found in the young stellar populations suggest a interaction with other system. This event would have triggered the main burst in the centre of the galaxy and expelled gas from the galaxy. The later recapture of this gas could explain the formation of shell like structures found by Coleman et al. (2004), clearly visible in the Figure 3.

References

Aparicio A. & Hidalgo S. L., 2009, AJ, 138, 558
Blumenthal G. R. et al. 1985, Nature, 313, 72
Carrera R. et al. 2008a, AJ, 135, 836
Coleman M. et al. 2004, AJ, 127, 832
del Pino, A., Hidalgo, S. L., Aparicio, A., et al. 2013, MNRAS, 433, 1505
Klypin, A. et al. 1999, ApJ, 522, 82
Kravtsov, A. V., Gnedin, O. Y., & Klypin, A. A. 2004, ApJ, 609, 482
Moore, B., Ghigna, S., Governato, F., et al. 1999, ApJ, 524, L19
Piatek S. et al. 2007, AJ, 133, 818
Stetson P. B., 2000, PASP, 112, 925
Stetson P. B., 2005, PASP, 117, 563